

## Thermal buckling resistance of simply supported FGM plates with parabolic-concave thickness variation

Fouad Benlahcen<sup>1,2a</sup>, Khalil Belakhdar<sup>\*1,3</sup>, Mohammed Sellami<sup>1b</sup> and Abdelouahed Tounsi<sup>3c</sup>

<sup>1</sup> Department of Science and Technology, University Centre of Tamanrasset, BP 10034 Sersouf, Tamanrasset, 11000, Algeria

<sup>2</sup> Laboratory of Science and Environment, University Centre of Tamanrasset, BP 10034 Sersouf, Tamanrasset, 11000, Algeria

<sup>3</sup> Laboratory of Materials and Hydrology, University of Sidi Bel Abbès, BP 89 Cité Ben M'hidi, Sidi Bel Abbès, 22000, Algeria

(Received February 6, 2018, Revised October 27, 2018, Accepted November 13, 2018)

**Abstract.** This research presents an investigation on the thermal buckling resistance of FGM plates having parabolic-concave thickness variation exposed to uniform and gradient temperature change. An analytical formulation is derived and the governing differential equation of thermal stability is solved numerically using finite difference method. A specific function of thickness variation is introduced where it controls the parabolic variation intensity of the thickness without changing the original material volume. The results indicated that the loss ratio in buckling resistance is the same for any gradient temperature profile. Influencing geometrical and material parameters on the loss ratio in the thermal resistance buckling are investigated which may help in design guidelines of such complex structures.

**Keywords:** FGM plate; thermal buckling; parabolic thickness variation; finite difference method

### 1. Introduction

In recent years, functionally graded materials (FGMs) have received a considerable attention in several engineering and industries applications such as spacecrafts, rocket engines and high temperature instruments, due to its high performance and resistance under thermal as well as mechanical loading. This type of composite materials is characterized by its properties that vary smoothly from one surface to the other surface. Generally, FGM are composed of metal and ceramic, where the smoothness is performed by gradually varying the volume fraction of the constituent materials. Such operation results a mixture characterized by an excellent mechanical properties under high temperature environment.

Many pieces of research work have been conducted to study the buckling behavior of FGM under mechanical and thermal loading by adopting different theories and assumptions. Zhao *et al.* (2009), Bourada *et al.* (2012), Zenkour and Sobhy (2010) Mozafari *et al.* (2010b, 2012a, b), Bouazza *et al.* (2009) carried out a thermal buckling behavior of a sigmoid distribution of FGM plates under uniform, linear, and sinusoidal temperature rise across the thickness based on FSDT. Matsunaga (2009) studied the thermal and mechanical analysis of FGM plates based on two-dimensional higher-order shear deformation theory

(HSDT) through using power series expansion to evaluate the displacements and stresses. Zenkour and Mashat (2010) analyzed the thermal buckling of FGM plates where they proposed a sinusoidal shear deformation plate theory. Through the comparison, their results found to be very close to that of different HSDT in the literature. Raki *et al.* (2012) proposed a closed-form solution based on HSDT to evaluate the critical buckling temperature under uniform and gradient temperature through the thickness. They compared their results with finite element method. Bouiadjra *et al.* (2012) presented a research work where they analyzed the thermal buckling of FGM plates by using a four-variable refined plate theory. Fekrar *et al.* (2013) investigated the thermal buckling of FGM plates having sigmoid material properties distribution exposed to uniform and sinusoidal temperature distribution through the thickness. The presented formulation was based on the FSDT. Kettaf *et al.* (2013) proposed in their research work a new hyperbolic displacement model to derive the thermal buckling of FGM sandwich. The presented formulation results only four governing equations. Fazzolari and Carrera (2014) studied the thermal stability of FGM sandwich plates under various nonlinear temperature distributions using refined quasi-3D Equivalent Single Layer and Zig-Zag plate models. Then they carried out parametric study to evaluate the effect of geometric and material parameters on the thermal buckling of FGM plates. Khalfi *et al.* (2014) presented a closed-form solution based on a refined and simple shear deformation theory to evaluate the critical buckling temperature of solar FGM plate resting on two-parameter Pasternak's foundations. They used the exact neutral surface position as reference to derive the stability equations. Similarly, Lee *et al.* (2016) considered that the material is asymmetry in the thickness direction. So, they took the neutral surface of

\*Corresponding author, Professor,  
E-mail: [be.khalil@gmail.com](mailto:be.khalil@gmail.com)

<sup>a</sup> Ph.D. Student

<sup>b</sup> Professor

<sup>c</sup> Professor

structures as reference to evaluate the thermal buckling behavior of FGM plates based on FSDT. Han *et al.* (2017) presented a theoretical formulation to study the buckling behavior of cylindrical shell structures with FGM coating under thermal loading. They used an empirical engineering formula in order to simplify the complex formulations that characterize the mathematical formulation of such structures. Yu *et al.* (2017) presented a numerical solution for buckling analysis of FGM rectangular and skew plates under combined thermal and mechanical loads. The numerical responses of buckling were computed using isogeometric analysis based on the FSDT. In addition, parametric studies were conducted to investigating the effects of various parameters on the thermo-mechanical buckling behavior. Kandasamy *et al.* (2016) carried a theoretical work to study the thermal buckling and vibration behavior of FGM structures including plates, cylindrical panels and shells in thermal environments by using the finite element method. Many examples were presented to demonstrate the accuracy of the proposed method and to study the effect of different material and geometrical parameters on the thermal stability of the FGM structures.

Recently, many researchers presented more simple and refined analytical procedure to study the thermal and mechanical stability of FGM plates (El-Hassar *et al.* 2016, Abdelhak *et al.* 2016, Bousahla *et al.* 2016, Chikh *et al.* 2017, Menasria *et al.* 2017, El-Haina *et al.* 2017). These pieces of research work focus on simplifying the conventional plate theories by reducing the number of unknown variables and equations with guarding the same level of accuracy. For instance, Elmoossouess *et al.* (2017) presented an accurate new HSDT that needs only four unknowns to study the thermal buckling of FGM sandwich plates with taking into account the variation of the thermal expansion coefficient through the thickness. Also, Houari *et al.* (2018) studied mechanical and thermal stability of FGM plates resting on elastic foundation using the hyperbolic shear deformation theory and stress function concept. Their presented procedure was less complicated than existing HSDT theories but with the same accuracy as the other high order theories.

According to the previously stated literature review, it should be noted that the thermal stability of FGM plates with constant thickness have been extensively studied. However, FGM plates having variable thickness have also attracted the attention of designers and researchers.

In general, geometrically complex FGM plates such as variable thickness plates become common in different engineering and industrial fields due to the design requirements. In spite of that, pieces of research work conducted to study the buckling of FGM plate with variable thickness are fewer in number compared to constant plate thickness. Rajasekaran and Wilson (2013) used the finite difference method to evaluate the exact buckling loads and vibration frequencies of variable thickness isotropic plates under different combinations of boundary conditions and loading. Pouladvand (2009) studied the buckling behavior of thin FGM rectangular plates with variable thickness exposed to different temperature distributions based on the on classical plate theory. Jalali *et al.* (2011) carried out an

investigation of mechanical buckling of circular sandwich plates under uniform radial compression loading. The plate has a homogenous core with variable thickness and FGM face sheet. The theoretical formulation was based on the FSDT. They solved the evaluated stability equations numerically. They found that the thickness variation has a significant effect of the critical buckling load. Mozafari *et al.* (Mozafari *et al.* 2010a, Mozafari and Ayob 2012) presented a piece of work to investigate the effect of thickness variation on the critical buckling temperature where the purpose of their studies was to improve the buckling resistance of the FGM plates. Ghomshei and Abbasi (2013) presented a numerical method by using finite element method to analyze the thermal buckling of FGM annular plates with variable thickness. Jabbarzadeh *et al.* (2013) presented an investigation on the thermal buckling behavior of FGM circular plates having variable thickness exposed to uniformly temperature distribution based on the FSDT. After evaluating the formulation of stability equations, they solved them numerically using pseudo-spectral method. In addition, they studied the effect of linear and parabolic thickness variations on the critical buckling temperature. Bouguenina *et al.* (2015) used a numerical solution based on finite difference method to investigate the thermal buckling behavior of simply supported FGM plates having variable thickness. They analyzed the effect of different geometrical and mechanical properties to evaluate their effect on the critical buckling of FGM plates having linear variable thickness. Le-Manh *et al.* (2017) studied nonlinear bending and buckling behavior of composite plates having variable thickness. The presented formulation is based on first-order shear deformation theory and it was found to be stable and accurate enough to predict the behavior of thin to moderately thick laminates plates.

The main objective of the present piece of research work is to study the temperature buckling resistance of FGM plates having parabolic-concave thickness variation. To attend this objective, the derived governing equation of the thermal stability is solved numerically by using the finite difference method in order to have the ability to include the thickness variation. Noting that such task is complex to be performed analytically. A special parabolic-concave function is developed to control the intensity of the parabolic-variation of the plate thickness but without changing its original material volume. A parametric study is conducted to investigate the effect of different parameters on the loss ratio in the critical buckling temperature.

## 2. Theoretical formulation

### 2.1 Material constitutive relations

We consider a functionally graded plate, composed of a mixture of ceramic and metal. The plate is subjected to a thermal load function  $T(x, y, z)$ . It is assumed that the composition properties of FGM vary through the thickness of the plate according a simple power-law function. The volume fractions of ceramic  $V_c$  and metal  $V_m$  are given as

$$\begin{cases} V_c = \left(\frac{z}{h} + \frac{1}{2}\right)^k ; & -\frac{h}{2} \leq z \leq \frac{h}{2} \\ V_m(z) + V_c(z) = 1 \end{cases} \quad (1)$$

$k$  is a parameter that controls the material variation profile, where  $0 \leq k \leq \infty$ .

The modulus  $E$  and the coefficient of thermal expansion  $\alpha$  are expressed as follows, noting that the Poisson's ratio is assumed constant  $\nu = 0.3$ .

$$\begin{cases} E(z) = E_c V_c + E_m (1 - V_c) \\ \alpha(z) = \alpha_c V_c + \alpha_m (1 - V_c) \end{cases} \quad (2)$$

### 2.2 Formulation of the stability equations

The displacement of the neutral plane of the FGM plate in  $x, y, z$  directions denote  $u, v, w$ , respectively.  $\phi_x$  and  $\phi_y$  denote the rotations of the mid-plate normals about  $x$  and  $y$  axes. Based on the first order shear deformation theory, the strains are given as

$$\begin{cases} \epsilon_x = u_{,x} + z\phi_{x,x} \\ \epsilon_y = v_{,y} + z\phi_{y,y} \\ \gamma_{xy} = u_{,y} + v_{,x} + z(\phi_{x,y} + \phi_{y,x}) \\ \gamma_{xz} = \phi_x + w_{,x} \\ \gamma_{zy} = \phi_y + w_{,y} \end{cases} \quad (3)$$

The stress-strain relationship according to Hook's law is

$$\begin{cases} \sigma_x = \frac{E}{1-\nu^2} (\epsilon_x + \nu\epsilon_y - (1+\nu)\alpha T) \\ \sigma_y = \frac{E}{1-\nu^2} (\epsilon_y + \nu\epsilon_x - (1+\nu)\alpha T) \\ \sigma_{xy} = \frac{E}{2(1+\nu)} \gamma_{xy} ; \sigma_{xz} = \frac{E}{2(1+\nu)} \gamma_{xz} \\ \sigma_{zy} = \frac{E}{2(1+\nu)} \gamma_{zy} \end{cases} \quad (4)$$

The forces and moments per unit length are given in terms of the stress components through the thickness as

$$\begin{cases} N_i = \int_{-h/2}^{h/2} \sigma_i dz ; i = x, y, xy \\ M_i = \int_{-h/2}^{h/2} \sigma_i z dz ; i = x, y, xy \\ Q_i = \int_{-h/2}^{h/2} \sigma_{iz} dz ; i = x, y \end{cases} \quad (5)$$

Substituting Eqs. (2)-(4) into Eq. (5) results

$$\begin{cases} N_x = \frac{E_1}{1-\nu^2} (u_{,x} + \nu v_{,y}) + \frac{E_2}{1-\nu^2} (\phi_{x,x} + \nu\phi_{y,y}) - \frac{\Phi}{1-\nu} \\ N_y = \frac{E_1}{1-\nu^2} (\nu u_{,x} + v_{,y}) + \frac{E_2}{1-\nu^2} (\nu\phi_{x,x} + \phi_{y,y}) - \frac{\Phi}{1-\nu} \\ N_{xy} = \frac{E_1}{2(1+\nu)} (u_{,y} + v_{,x}) + \frac{E_2}{2(1+\nu)} (\phi_{x,y} + \phi_{y,x}) \\ M_x = \frac{E_2}{1-\nu^2} (u_{,x} + \nu v_{,y}) + \frac{E_3}{1-\nu^2} (\phi_{x,x} + \nu\phi_{y,y}) - \frac{\Theta}{1-\nu} \\ M_y = \frac{E_2}{1-\nu^2} (\nu u_{,x} + v_{,y}) + \frac{E_3}{1-\nu^2} (\nu\phi_{x,x} + \phi_{y,y}) - \frac{\Theta}{1-\nu} \\ M_{xy} = \frac{E_2}{2(1+\nu)} (u_{,y} + v_{,x}) + \frac{E_3}{2(1+\nu)} (\phi_{x,y} + \phi_{y,x}) \\ Q_x = \frac{E_1}{2(1+\nu)} (\phi_x + w_{,x}) \\ Q_y = \frac{E_1}{2(1+\nu)} (\phi_y + w_{,y}) \end{cases} \quad (6)$$

Where

$$(E_1, E_2, E_3) = \int_{-h/2}^{h/2} (1, z, z^2) E(z) dz \quad (7)$$

$$(\Phi, \Theta) = \int_{-h/2}^{h/2} E(z) \alpha(z) T(z) (1, z) dz \quad (8)$$

The nonlinear equations of equilibrium are given according to Von Karman's tensor by

$$\begin{cases} N_{x,x} + N_{xy,y} = 0 \\ N_{y,y} + N_{xy,x} = 0 \\ M_{x,x} + M_{xy,y} - Q_x = 0 \\ M_{xy,x} + M_{y,y} - Q_y = 0 \\ Q_{x,x} + Q_{y,y} + q + N_x w_{,xx} + N_y w_{,yy} + 2 N_{xy} w_{,xy} = 0 \end{cases} \quad (9)$$

By eliminating the variables  $u, v, \phi_x, \phi_y$  through manipulating Eqs. (6) and (9), we get

$$\begin{aligned} \nabla^4 w + \frac{2(1+\nu)}{E_1} \nabla^2 (N_x w_{,xx} + N_y w_{,yy} + 2 N_{xy} w_{,xy} + q) \\ - \frac{E_1(1-\nu^2)}{E_1 E_3 - E_2^2} (N_x w_{,xx} + N_y w_{,yy} + 2 N_{xy} w_{,xy} + q) = 0 \end{aligned} \quad (10)$$

The critical equilibrium method is used to establish the stability equations. So, by assuming that the state of stable equilibrium of a general plate under thermal load may be designated by the deflection  $w_0$ . The displacement of the neighboring state is given by

$$\Delta w = w_0 + w_1 \quad (11)$$

where  $w_1$  is an arbitrarily small increment of displacement. By substituting Eq. (11) into Eq. (10) and re-evaluating the original equation, results in the following stability equation

$$\begin{aligned} \nabla^4 w_1 + \frac{2(1+\nu)}{E_1} \nabla^2 (N_x^0 w_{1,xx} + N_y^0 w_{1,yy} + 2 N_{xy}^0 w_{1,xy}) \\ - \frac{E_1(1-\nu^2)}{E_1 E_3 - E_2^2} (N_x^0 w_{1,xx} + N_y^0 w_{1,yy} + 2 N_{xy}^0 w_{1,xy}) = 0 \end{aligned} \quad (12)$$

where,  $N_x^0$ ,  $N_y^0$  and  $N_{xy}^0$  are the pre-buckling force resultants.

Finally, the critical buckling temperature difference  $\Delta T_{cr}$  can be evaluated after determination of the pre-buckling thermal forces. The latter is found by solving the membrane form of equilibrium equations, as

$$\begin{cases} N_x^0 = -\frac{\Phi}{1-\nu} \\ N_y^0 = -\frac{\Phi}{1-\nu} \\ N_{xy}^0 = 0 \end{cases} \quad (13)$$

Substituting Eq. (13) into Eq. (12), we obtain

$$\nabla^4 w_1 - \frac{2(1+\nu)}{E_1} \frac{\Phi}{1-\nu} \nabla^4 w_1 + \frac{E_1(1-\nu^2)}{E_1 E_3 - E_2^2} \frac{\Phi}{1-\nu} \nabla^2 w_1 = 0 \quad (14)$$

**3. Finite difference solution**

The fourth order differential equation presented by Eq. (14) can be solved numerically using finite difference method. To do that, we consider a rectangular FGM plate meshed into  $n \times m$  nodes spaced by  $\Delta h$  in  $x$  and  $y$  directions, as shown in Fig. (1).

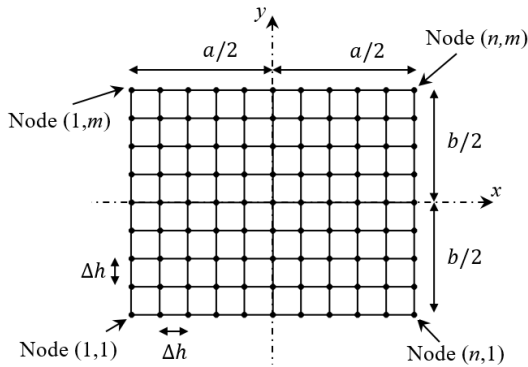


Fig. 1 Finite difference mesh of the plate

The governing equation given by Eq. (14) is simplified as

$$\nabla^4 w_1(1 + D_1 \Phi) + D_2 \Phi \nabla^2 w_1 = 0 \quad (15)$$

Where

$$\begin{cases} D_1 = -\frac{2(1+\nu)}{E_1(1-\nu)} \\ D_2 = \frac{E_1(1-\nu^2)}{(E_1 E_3 - E_2^2)(1-\nu)} \end{cases} \quad (16)$$

In finite difference format, Eq. (14) is written as

$$\begin{aligned} & \left( \frac{20}{\Delta^2} (D_1 \Phi + 1) - 4D_2 \Phi \right) w_{1(i,j)} \\ & + \left( -\frac{8}{\Delta^2} (D_1 \Phi + 1) + D_2 \Phi \right) \left( w_{1(i,j-1)} + w_{1(i,j+1)} \right) \\ & + \left( \frac{2}{\Delta^2} (D_1 \Phi + 1) \right) \left( w_{1(i-1,j-1)} + w_{1(i-1,j+1)} \right) \\ & + \left( \frac{1}{\Delta^2} (D_1 \Phi + 1) \right) \left( w_{1(i,j-2)} + w_{1(i,j+2)} \right) \\ & + \left( w_{1(i-1,j)} + w_{1(i+1,j)} \right) \\ & + \left( w_{1(i-2,j)} + w_{1(i+2,j)} \right) = 0 \end{aligned} \quad (17)$$

This mesh is applied at nodes with coordinates  $(i = 2..n-1, j = 2..m-1)$ . Noting that this operation will result virtual nodes along the lines  $(i = 2, i = n-1, j = 2, j = m-1)$ .

Since the plate is simply supported, the boundary conditions are given as follows

$$\begin{cases} \text{at } x = \pm a/2: w_1 = 0; M_{x1} = 0 \\ \text{at } y = \pm b/2: w_1 = 0; M_{y1} = 0 \end{cases} \quad (18)$$

So, the displacements along the edges are equal to zero as

$$\begin{aligned} w_{1(i,j)} = 0 & \text{ at } [i = (1, n), j = (1..m)] \\ & \text{and } [i = (1..n), j = (1, m)] \end{aligned} \quad (19)$$

In addition, the moments along the edges are nulls. By expressing the moments in terms of the deflections  $w_1$  along the edge, the virtual nodes are simply eliminated resulting the following system of simultaneous  $(n-2) \times (m-2)$  equations

$$\begin{bmatrix} \left( \frac{18}{\Delta^2} (D_1 \Phi + 1) \right) & \left( -\frac{8}{\Delta^2} (D_1 \Phi + 1) \right) & \left( \frac{1}{\Delta^2} (D_1 \Phi + 1) \right) & \dots \\ \left( -\frac{8}{\Delta^2} (D_1 \Phi + 1) \right) & \left( \frac{19}{\Delta^2} (D_1 \Phi + 1) \right) & \left( -\frac{8}{\Delta^2} (D_1 \Phi + 1) \right) & \dots \\ \left( \frac{1}{\Delta^2} (D_1 \Phi + 1) \right) & \left( -\frac{8}{\Delta^2} (D_1 \Phi + 1) \right) & \left( \frac{20}{\Delta^2} (D_1 \Phi + 1) \right) & \dots \\ \vdots & \vdots & \vdots & \ddots & \vdots \\ \dots & \dots & \dots & \dots & \left( \frac{20}{\Delta^2} (D_1 \Phi + 1) \right) & \left( -\frac{8}{\Delta^2} (D_1 \Phi + 1) \right) & \left( \frac{1}{\Delta^2} (D_1 \Phi + 1) \right) & \dots & \dots & \dots & \dots \\ \dots & \dots & \dots & \dots & \left( -\frac{8}{\Delta^2} (D_1 \Phi + 1) \right) & \left( \frac{20}{\Delta^2} (D_1 \Phi + 1) \right) & \left( -\frac{8}{\Delta^2} (D_1 \Phi + 1) \right) & \dots & \dots & \dots & \dots \\ \dots & \dots & \dots & \dots & \left( \frac{1}{\Delta^2} (D_1 \Phi + 1) \right) & \left( -\frac{8}{\Delta^2} (D_1 \Phi + 1) \right) & \left( \frac{20}{\Delta^2} (D_1 \Phi + 1) \right) & \dots & \dots & \dots & \dots \\ \vdots & \vdots & \vdots & \ddots & \vdots \end{bmatrix} \times \begin{bmatrix} w_{1(2,2)} \\ w_{1(3,2)} \\ \vdots \\ w_{1(i-1,j)} \\ w_{1(i,j)} \\ \vdots \\ w_{1(i+1,j)} \\ \vdots \end{bmatrix} = \begin{bmatrix} 0 \\ 0 \\ \vdots \\ 0 \\ 0 \\ \vdots \\ 0 \\ \vdots \end{bmatrix} \quad (20)$$

### 3.1 Determination of the critical temperature

The critical buckling temperature is evaluated for two cases of temperature rise; uniform temperature rise and gradient temperature rise, the later represents linear and non-linear temperature variation through the thickness.

*Case 1: Uniform Temperature Rise:* In this case, the plate is assumed to have an initial uniform temperature  $T_i$ . The temperature is raised uniformly through the thickness to a final value  $T_f$  in which the plate buckles. The buckling temperature difference is simply defined as

$$T(z) = T_f - T_i = \Delta T \quad (21)$$

Substituting Eq. (21) into Eq. (8) and Eq. (15) we get

$$\Delta T = -\frac{\nabla^4 w_1}{\xi_0(D_1 \nabla^4 w_1 + D_2 \nabla^2 w_1)} \quad (22)$$

$$\xi_0 = \int_{-h/2}^{h/2} \alpha(z)E(z)dz \quad (23)$$

*Case 2: Gradient Temperature Rise:* we assume that the temperature of top metallic surface is  $T_m$ , and the temperature varies nonlinearly through the thickness from the top metallic surface temperature  $T_m$  to the bottom surface ceramic temperature  $T_c$  in which the plate buckles. The temperature variation is given by the following equation

$$T(z) = \Delta T \cdot \left(\frac{z}{h} + \frac{1}{2}\right)^\beta + T_m \quad (24)$$

Where  $\Delta T$  is the buckling temperature difference  $\Delta T = T_c - T_m$  and  $\beta$  is the exponent of the variation. Noting that  $\beta = 1$  represents a linear variation of the temperature through the plate thickness. While when  $\beta > 1$  represents a nonlinear temperature variation.

By substituting (24) into Eq. (8) and Eq. (15) we get

$$\Delta T = \frac{((-D_1 T_m \xi_0 - 1)\nabla^4 w_1 - D_2 T_m \xi_0 \nabla^2 w_1)}{\xi_1(D_1 \nabla^4 w_1 + D_2 \nabla^2 w_1)} \quad (25)$$

$$\xi_1 = \int_{-h/2}^{h/2} \alpha(z)E(z) \left(\frac{z}{h} + \frac{1}{2}\right)^\beta dz \quad (26)$$

### 3.2 Evaluation of $\Delta T_{cr}$

The homogeneous simultaneous equations represented by Eq. (20) cannot be solved because it contains of the unknown temperature distribution  $T(z)$ . This problem is solved by using the trial and error technique as follows:

- (1) In the first trial, an initial value equals to unity is assigned to  $\Delta T$ , After solving the system of equations, the first mode shape  $w_1^{(1)}$  is used to

calculate the critical buckling temperature  $\Delta T_{cr1}$  using Eq. (22) or Eq. (25). Noting that these equations are calculated numerically using their finite difference format.

- (2) The obtained  $\Delta T_{cr1}$  is used for another iteration to solve the simultaneous equations Eq. (20) where a new critical temperature difference  $\Delta T_{cr2}$  is obtained.
- (3) Step 2 is repeated successively until the following criteria is satisfied

$$\frac{\Delta T_{cr_i} - \Delta T_{cr_{i-1}}}{\Delta T_{cr_i}} \leq 10^{-5} \quad (27)$$

## 4. Validation of the finite difference method

In order to validate the present numerical method, the predicted critical buckling temperature of simply supported FG plates under uniform, linear, and nonlinear temperature change through the thickness are compared with the literature.

Assuming FGM plate consists of aluminum and alumina where The Young's modulus and the coefficient of thermal expansion for alumina are  $E_c = 380 \text{ GPa}$ ,  $\alpha_c = 7.4 \times 10^{-6}/^\circ\text{C}$  and for the aluminum are  $E_m = 70 \text{ GPa}$ ,  $\alpha_m = 23 \times 10^{-6}/^\circ\text{C}$ , respectively, while Poisson's ratio is assumed to be constant for both metal and ceramic with  $\nu = 0.3$ . For all the analysis, it is assumed that the initial temperature  $T_i = 5^\circ\text{C}$  for the uniform temperature rise case, while for gradient temperature rise case, the metal-rich surface temperature of the plate is assumed to be  $T_m = 5^\circ\text{C}$ .

Tables 1, 2, and 3 summarize the critical thermal buckling for simply supported rectangular plate under uniform, linear, and nonlinear temperature change, respectively, for different values of the material distribution parameter  $k$  and aspect ratio  $a/b$ .

The present results in Tables 1-3 are given for different mesh sizes ( $a/\Delta h = 10, 20, 30, 40$ ) to test the convergence of the finite difference solution. Additionally, to enhance the accuracy of the predicted results, Richardson's extrapolation formula is adopted, which is expressed as Szilard (2004)

$$\Delta T_{cr}^{[ex]} = \Delta T_{cr}^{[40]} + \frac{\Delta T_{cr}^{[40]} - \Delta T_{cr}^{[20]}}{2^\mu - 1} \quad (28)$$

Where  $\Delta T_{cr}^{[ex]}$  is the extrapolated value,  $\Delta T_{cr}^{[20]}$  and  $\Delta T_{cr}^{[40]}$  are the values of critical temperature obtained by using mesh size  $a/\Delta h = 20$  and  $a/\Delta h = 40$ , respectively.  $\mu = 2$  is the exponent value which depends on the convergence characteristics of the numerical method.

According to Tables 1-3, it can be observed that the present results are in excellent agreement with FSDT theory presented by Bouazza *et al.* (2009) and Zenkour and Mashat (2010), which validate the present numerical method.

Table 1 Critical buckling temperature ( $^{\circ}\text{C}$ ) of FG plate under uniform temperature rise for different values of power law index  $k$  and aspect ratio  $a/b$  with  $a/h = 100$ 

	Mesh $a/\Delta h$	$a/b = 1$	$a/b = 2$	$a/b = 3$	$a/b = 4$	
$k = 0$	10	16.952	42.403	84.664	143.654	
	20	17.057	42.625	85.140	144.491	
	Present	30	17.076	42.667	85.229	144.647
		40	17.083	42.681	85.260	144.701
		$\Delta T_{cr}^{[ex]}$	<b>17.092</b>	<b>42.700</b>	<b>85.299</b>	<b>144.771</b>
		Ref. (Bouazza <i>et al.</i> 2009)	17.091	42.698	85.295	144.764
	Ref. (Zenkour and Mashat 2010)	17.089	42.688	85.255	144.649	
$k = 1$	10	7.876	19.703	39.347	66.779	
	20	7.925	19.806	39.568	67.169	
	Present	30	7.934	19.825	39.609	67.241
		40	7.937	19.832	39.624	67.266
		$\Delta T_{cr}^{[ex]}$	<b>7.941</b>	<b>19.841</b>	<b>39.642</b>	<b>67.299</b>
		Ref. (Bouazza <i>et al.</i> 2009)	7.941	19.840	39.640	67.296
	Ref. (Zenkour and Mashat 2010)	7.940	19.836	39.625	67.251	
$k = 5$	10	7.204	18.018	35.976	61.039	
	20	7.248	18.113	36.178	61.395	
	Present	30	7.257	18.131	36.216	61.461
		40	7.259	18.137	36.229	61.484
		$\Delta T_{cr}^{[ex]}$	<b>7.263</b>	<b>18.145</b>	<b>36.246</b>	<b>61.514</b>
		Ref. (Bouazza <i>et al.</i> 2009)	7.262	18.142	36.241	61.506
	Ref. (Zenkour and Mashat 2010)	7.262	18.138	36.224	61.456	
$k = 10$	10	7.406	18.522	36.976	62.723	
	20	7.452	18.619	37.184	63.088	
	Present	30	7.460	18.637	37.222	63.156
		40	7.463	18.644	37.236	63.179
		$\Delta T_{cr}^{[ex]}$	<b>7.467</b>	<b>18.652</b>	<b>37.253</b>	<b>63.210</b>
		Ref. (Bouazza <i>et al.</i> 2009)	7.465	18.648	37.245	63.196
	Ref. (Zenkour and Mashat 2010)	7.464	18.643	37.225	63.138	

## 5. FGM plate with parabolic thickness variation

As mentioned previously, the objective of this study deals with investigating the thermal buckling resistance simply supported FGM plates with parabolic thickness variation. The proposed thickness variation function changes only the intensity of the parabolic variation while it conserves the original material volume of the plate. Two types of thickness variation have been studied; parabolic variation in one direction, and parabolic variation in both directions, as shown in Fig. 2.

In case of one direction, the plate thickness becomes a function in terms of  $x$  which is derived according to the following general parabolic function

$$H(x) = -\frac{4}{a^2}(e_0 - e_1)x^2 + e_0 \quad (29)$$

Where  $e_0$  is the thickness at the plate mid center ( $x = 0$ ), and  $e_1$  is the thickness at the plate edges i.e., at

$$x = (-a/2, a/2).$$

Let  $V_0$  be the volume of constant thickness plate (original plate) with has a constant thickness  $h$  and let  $V_1$  be the volume of variable-thickness plate, where

$$V_0 = a \cdot b \cdot h \quad (30)$$

$$V_1 = a \cdot b \left( \frac{2}{3}(e_0 - e_1) + e_1 \right) \quad (31)$$

By maintaining the same volumes of both plates as  $V_0 = V_1$ , we get

$$e_1 + 2e_0 = 3h \quad (32)$$

Expressing  $e_0$  in terms of  $e_1$  as

$$e_1 = \eta \cdot e_0 \quad (33)$$

Table 2 Critical buckling temperature (°C) of FG plate under linear temperature rise for different values of power law index  $k$  and aspect ratio  $a/b$  with  $a/h = 100$

	Mesh	$a/\Delta h$	$a/b = 1$	$a/b = 2$	$a/b = 3$	$a/b = 4$
$k = 0$	Present	10	23.904	74.805	159.327	277.309
		20	24.114	75.251	160.280	278.983
		30	24.153	75.333	160.457	279.294
		40	24.166	75.362	160.519	279.403
		$\Delta T_{cr}^{[ex]}$	<b>24.184</b>	<b>75.399</b>	<b>160.599</b>	<b>279.543</b>
	Ref. (Bouazza <i>et al.</i> 2009)		17.091	24.182	75.395	160.590
Ref. (Zenkour and Mashat 2010)		17.089	24.179	75.375	160.510	
$k = 1$	Present	10	5.394	85.749	64.416	115.865
		20	5.485	27.768	64.831	116.595
		30	5.502	27.804	64.909	116.731
		40	5.508	27.817	64.936	116.778
		$\Delta T_{cr}^{[ex]}$	<b>5.516</b>	<b>27.833</b>	<b>64.970</b>	<b>116.839</b>
	Ref. (Bouazza <i>et al.</i> 2009)		7.941	5.515	27.832	64.967
Ref. (Zenkour and Mashat 2010)		7.940	5.514	27.824	64.938	
$k = 5$	Present	10	3.793	22.409	53.319	96.461
		20	3.870	22.572	53.667	97.073
		30	3.884	22.602	53.732	97.187
		40	3.889	22.612	53.754	97.227
		$\Delta T_{cr}^{[ex]}$	<b>3.896</b>	<b>22.626</b>	<b>53.783</b>	<b>97.278</b>
	Ref. (Bouazza <i>et al.</i> 2009)		7.262	3.894	22.622	53.775
Ref. (Zenkour and Mashat 2010)		7.262	3.893	22.614	53.745	
$k = 10$	Present	10	4.263	23.963	56.664	102.291
		20	4.344	24.135	57.033	102.938
		30	4.360	24.167	57.101	103.059
		40	4.365	24.178	57.125	103.101
		$\Delta T_{cr}^{[ex]}$	<b>4.371</b>	<b>24.193</b>	<b>57.156</b>	<b>103.155</b>
	Ref. (Bouazza <i>et al.</i> 2009)		7.465	4.369	24.185	57.140
Ref. (Zenkour and Mashat 2010)		7.464	4.367	24.176	57.104	

Where  $\eta$  represents the plate edge-to-mid center thickness ratio. Noting that  $\eta > 1$  corresponds to parabolic-concave variation.

Substituting Eqs. (32) and (33) in Eq. (29); we obtain the thickness variation function as

$$H(x) = \frac{3h}{2 + \eta} \left( \frac{4(\eta - 1)}{a^2} x^2 + 1 \right) \quad (34)$$

Thus, the thickness variation function is expressed by one parameter  $\eta$  that controls the intensity of the parabolic variation and keeps the volume of the new plate equal to that of the original plate as shown in Fig. 2.

In case of plate having variable thickness in two directions, the thickness function is derived from the general parabolic

$$H(x, y) = \frac{16(e_0 - e_1)}{a^2 b^2} x^2 y^2 - \frac{4(e_0 - e_1)}{a^2} x^2 - \frac{4(e_0 - e_1)}{b^2} y^2 + e_0 \quad (35)$$

Let  $V_2$  be the volume of this plate which is given as follows

$$V_2 = a \cdot b \left( \frac{4}{9} (e_0 - e_1) + e_1 \right) \quad (36)$$

By making  $V_0 = V_2$ , we get

$$5e_1 + 4e_0 = 9h \quad (37)$$

Expressing  $e_0$  in terms of  $e_1$  as

$$e_1 = \eta \cdot e_0 \quad (38)$$

Substituting Eqs. (37) and (38) into Eq. (35), the function  $H(x, y)$  can be written as follows

$$H(x, y) = \frac{9h}{4 + 5\eta} \left( 4(\eta - 1) \left( \frac{x^2}{a^2} + \frac{y^2}{b^2} - 4 \frac{x^2 y^2}{a^2 b^2} \right) + 1 \right) \quad (39)$$

Similarly, the intensity parameter  $\eta$  controls the

Table 3 Critical buckling temperature ( $\Delta T \times 10^{-3} \text{ }^\circ\text{C}$ ) of FG plate under uniform temperature rise for different values of power law index  $k$  and aspect ratio  $a/b$  with  $a/h = 10$

	Mesh $\frac{a}{\Delta h}$	$a/b = 1$			$a/b = 2$			$a/b = 3$			
		$\beta = 2$	$\beta = 5$	$\beta = 10$	$\beta = 2$	$\beta = 5$	$\beta = 10$	$\beta = 2$	$\beta = 5$	$\beta = 10$	
$k = 0$	Present	10	4.846	9.692	17.766	11.390	22.778	41.753	20.628	41.254	75.620
		20	4.875	9.750	17.871	11.443	22.886	41.950	20.722	41.443	75.966
		30	4.880	9.760	17.891	11.453	22.906	41.987	20.740	41.478	76.030
		40	4.882	9.764	17.898	11.457	22.913	41.999	20.746	41.490	76.052
		$\Delta T_{cr}^{[ex]}$	<b>4.885</b>	<b>9.769</b>	<b>17.907</b>	<b>11.461</b>	<b>22.922</b>	<b>42.016</b>	<b>20.754</b>	<b>41.506</b>	<b>76.081</b>
	Ref. (Bouazza <i>et al.</i> 2009)	4.884	9.769	17.910	11.461	22.922	42.024	20.753	41.507	76.095	
	Ref. (Zenkour and Mashat 2010)	4.841	9.682	17.750	11.225	22.449	41.157	19.992	39.984	73.304	
$k = 1$	Present	10	2.106	4.316	8.186	5.007	10.263	19.464	9.200	18.857	35.762
		20	2.119	4.342	8.235	5.031	10.312	19.557	9.244	18.946	35.931
		30	2.121	4.347	8.244	5.036	10.322	19.575	9.252	18.963	35.962
		40	2.122	4.349	8.247	5.037	10.325	19.581	9.255	18.969	35.973
		$\Delta T_{cr}^{[ex]}$	<b>2.123</b>	<b>4.351</b>	<b>8.251</b>	<b>5.039</b>	<b>10.329</b>	<b>19.589</b>	<b>9.258</b>	<b>18.976</b>	<b>35.987</b>
	Ref. (Bouazza <i>et al.</i> 2009)	2.123	4.351	8.253	5.039	10.329	19.591	9.258	18.976	35.993	
	Ref. (Zenkour and Mashat 2010)	2.107	4.318	8.190	4.950	10.146	19.244	8.962	18.368	34.840	
$k = 5$	Present	10	1.616	2.886	5.064	3.802	6.788	11.911	6.875	12.275	21.539
		20	1.626	2.903	5.094	3.820	6.820	11.967	6.907	12.330	21.637
		30	1.628	2.906	5.100	3.823	6.825	11.977	6.913	12.341	21.656
		40	1.628	2.907	5.102	3.824	6.828	11.981	6.915	12.344	21.662
		$\Delta T_{cr}^{[ex]}$	<b>1.629</b>	<b>2.909</b>	<b>5.104</b>	<b>3.826</b>	<b>6.830</b>	<b>11.986</b>	<b>6.917</b>	<b>12.349</b>	<b>21.670</b>
	Ref. (Bouazza <i>et al.</i> 2009)	1.629	2.908	5.104	3.825	6.825	11.985	6.916	12.348	21.670	
	Ref. (Zenkour and Mashat 2010)	1.614	2.882	5.057	3.744	6.685	11.732	6.657	11.885	20.857	
$k = 10$	Present	10	1.702	2.928	4.844	3.972	6.833	11.304	7.105	12.223	20.219
		20	1.712	2.946	4.873	3.990	6.865	11.356	7.136	12.277	20.309
		30	1.714	2.949	4.878	3.994	6.871	11.366	7.142	12.287	20.326
		40	1.715	2.950	4.880	3.995	6.873	11.369	7.144	12.291	20.331
		$\Delta T_{cr}^{[ex]}$	<b>1.716</b>	<b>2.951</b>	<b>4.882</b>	<b>3.996</b>	<b>6.876</b>	<b>11.374</b>	<b>7.147</b>	<b>12.295</b>	<b>20.339</b>
	Ref. (Bouazza <i>et al.</i> 2009)	1.715	2.951	4.881	3.995	6.874	11.371	7.145	12.292	20.335	
	Ref. (Zenkour and Mashat 2010)	1.697	2.920	4.831	3.902	6.712	11.104	6.851	11.786	19.498	

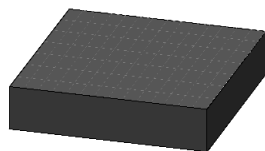


Plate with constant thickness variation (with V0)

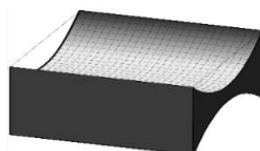


Plate with parabolic thickness variation in one direction (with V1 = V0)

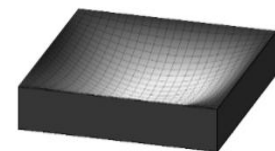


Plate with parabolic thickness variation in two direction (with V2 = V0)

Fig. 2 plates having parabolic thickness-variation profile

intensity of the parabolic variation in the two directions and keeps the volume of the new plate equal to that of the original constant-thickness plate as clarified in Fig. 2.

5.1 Finite difference considerations

In the finite difference idealization in case of variable thickness plate, it is assumed that at each discrete  $Node_{(i,j)}$

the thickness is constant given by  $h_{(i,j)}$  as shown in Fig. (3). The value of  $h_{(i,j)}$  is simply calculated by substituting the Node's coordinates in the thickness function  $H(x)$  or  $H(x, y)$  (Eq. (29) or Eq. (34)). In this case, the coordinate  $z_{(i,j)}$  at each  $Node_{(i,j)}$  varies in its specific domain:  $[-h_{(i,j)}/2, h_{(i,j)}/2]$ . According to Eq. (1) the material distribution profile through the thickness will be the same at

each node since the volume fractions of the material constituents is dependent on the ratio  $z/h$ , i.e.,  $z_{(i,j)}/h_{(i,j)} = [-1, +1]$ .

Based on that, all the equations containing the thickness parameters  $h$  such as Eq. (7), they are calculated by using the constant value  $h_{(i,j)}$ . In addition, the integration expressions through the thickness are evaluated using trapezoidal rule noting that each thickness  $h_{(i,j)}$  is divided into 2000 layers.

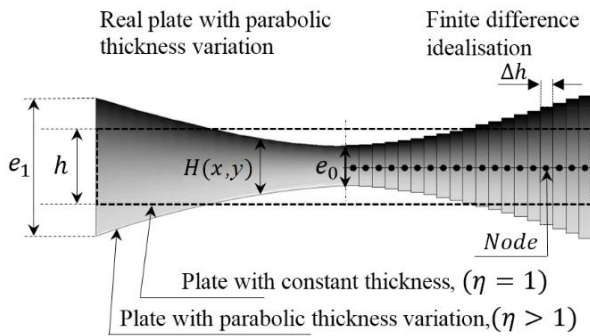


Fig. 3 Finite difference idealisation of FGM plate with parabolic thickness variation

### 6. Results and discussion

The effect of the parabolic variation intensity parameter  $\eta$  (edge-to-mid thickness ratio) on the thermal buckling of FGM plates exposed to uniform, linear, and nonlinear temperature rise through the thickness, are shown in Figs. 4-6.

The general note that can be observed from these figures is that varying the thickness geometry of the plate to fit a parabolic-concave shape decreases significantly its critical thermal buckling temperature especially when the thickness variation is applied in the two directions. In addition, the critical buckling temperature of FGM plate having parabolic-thickness variation is affected by the material

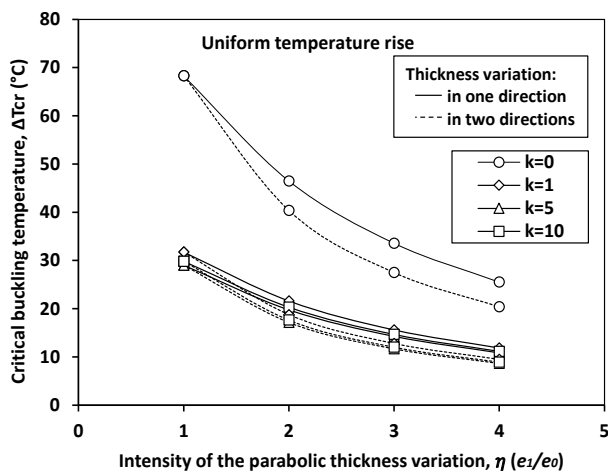


Fig. 4 Effect of the parabolic intensity variation parameter  $\eta$  on the critical buckling temperature of FGM square plate under uniform temperature rise

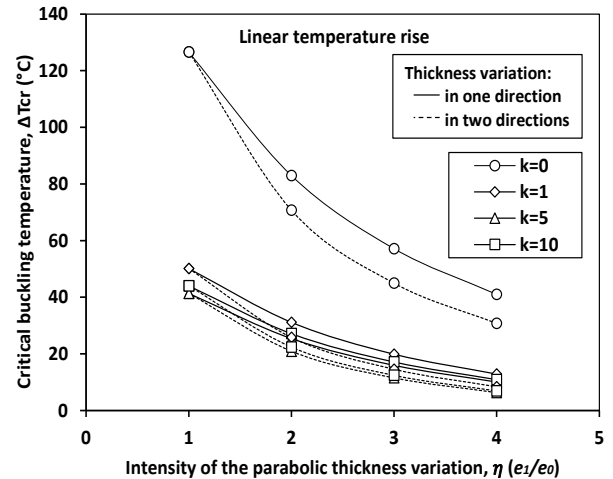


Fig. 5 Effect of the parabolic intensity variation parameter  $\eta$  on the critical buckling temperature of FGM square plate under linear temperature rise

distribution profile where, as the value of the power law index  $k$  increases the critical buckling temperature decreases. This is because plate with high metal content has lower stiffness with higher thermal expansion compared to the one with high ceramic content.

Figs. 7 and 8 represent the loss ratio of thermal buckling resistance in FGM plates with parabolic thickness variation in terms of  $\eta$ , exposed to uniform and gradient temperature rise, respectively. It is meant by the loss ratio of the buckling resistance; the degradation ratio of the critical buckling load of FGM plate with variable thickness ( $\eta > 1$ ) with respect to that of the original constant plate thickness ( $\eta = 1$ ). The loss ratio is simply calculated as follows

$$\text{The loss ratio in } \Delta T_{cr} = \left( \frac{\Delta T_{cr}(\text{constant thickness}) - \Delta T_{cr}(\text{variable thickness})}{\Delta T_{cr}(\text{constant thickness})} \right) \quad (40)$$

Figs. 7 and 8 show that the loss ratio in the critical buckling temperature increases as the parabolic intensity of the thickness variation parameter  $\eta$  increases. This is justified by the fact that the increase in the value of  $\eta$  helps to the occurrence of buckling since it reduces the thickness at the plate-middle where the buckling starts to develop.

Under uniform temperature rise, as shown in Fig. 7, the relationship between the loss ratio of the thermal buckling resistance and the parabolic variation intensity  $\eta$  is not affected by the variation the volume fraction of the constituent materials  $k$ , which means that whatever the value of  $k$  is, the loss ratio in the critical buckling temperature is the same. In this case where  $a/h = 50$ , it can be observed that, the loss ratio in the critical buckling temperature in homogenous plate and that in FGM plate which has the same geometric properties and thickness variation intensity, is the same. In other words, the loss ratio under uniform temperature rise is dependent on the geometrical properties of the thickness variation but not on the material variation profile. However, when the plate is

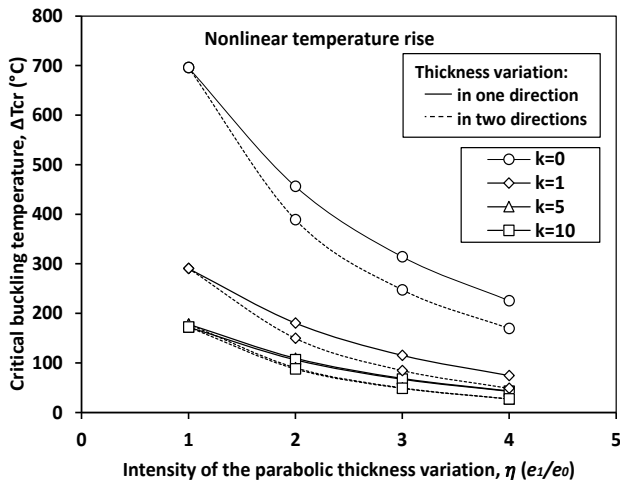


Fig. 6 Effect of the parabolic intensity variation parameter  $\eta$  on the critical buckling temperature of FGM square plate under nonlinear temperature rise

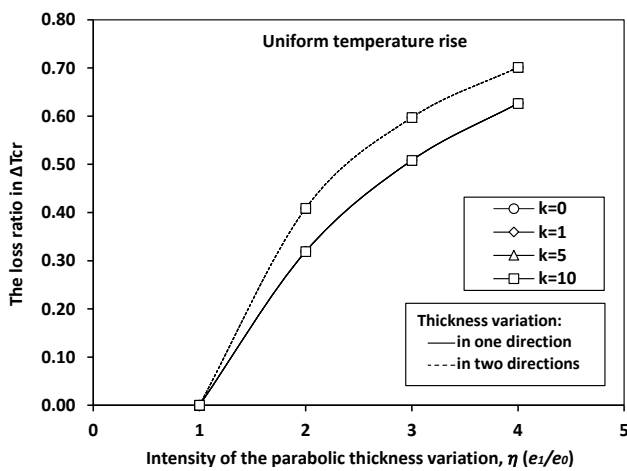


Fig. 7 The loss ratio in the critical buckling temperature versus the parabolic intensity variation parameter  $\eta$  in FGM plate exposed to uniform temperature rise

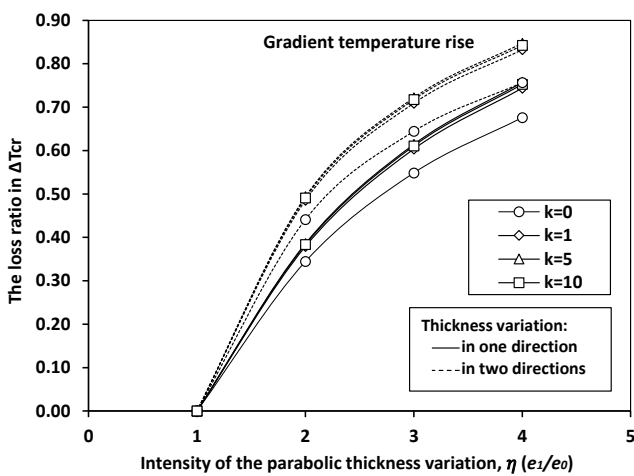


Fig. 8 The loss ratio in the critical buckling temperature versus the parabolic intensity variation parameter  $\eta$  in FGM plate exposed to gradient temperature rise

exposed to gradient temperature rise through to thickness, the loss ratio appears to be affected by the material distribution profile ( $k$ ), as shown in Fig. 8, where the loss ratio in the thermal resistance increases as the parabolic variation intensity  $\eta$  and the material distribution  $k$  increase. This relationship is the same for any applied gradient temperature distribution profile (linear or nonlinear).

The effect of the side-to-thickness ratio  $a/h$  on the loss ratio in the critical buckling temperature of simply supported FGM plates having parabolic thickness variation with intensity  $\eta = 2$  exposed to uniform temperature rise, is presented in Fig. 9. The figure clearly show that the loss ratio in the critical buckling temperature is almost constant for  $a/h < 20$ . Where it equals to 41% and 32% in case of thickness variation in one and two directions, respectively. For thick plates with  $a/h < 50$ , the loss ratio becomes slightly sensible to the material distribution parameter  $k$ . This sensibility increases as the  $a/h$  decreases.

According to what is stated in Fig. 7, it is concluded that plates with side-to-thickness ratio  $a/h < 20$  exposed to uniform temperature rise will loss the same ratio of the buckling resistance if they have the same geometric properties including the thickness variation intensity. This loss ratio is highly independent to the material distribution profile.

The effect of the side-to-thickness ratio  $a/h$  on the loss ratio of the critical buckling temperature of simply supported FGM plate having parabolic thickness variation with intensity  $\eta = 2$  exposed to gradient temperature rise (linear and nonlinear) through the thickness, is presented in Fig. 10.

The results indicate that the loss ratio is the same for any gradient temperature profile through the thickness. In addition, the loss ratio in the critical buckling temperature starts to increase as the side-to-thickness ratio increases but with high rate for higher values of the material distribution parameter  $k$ . This is due to the combined effect of the low stiffness in both geometrical and material properties. The variation of the loss ratio in the critical buckling

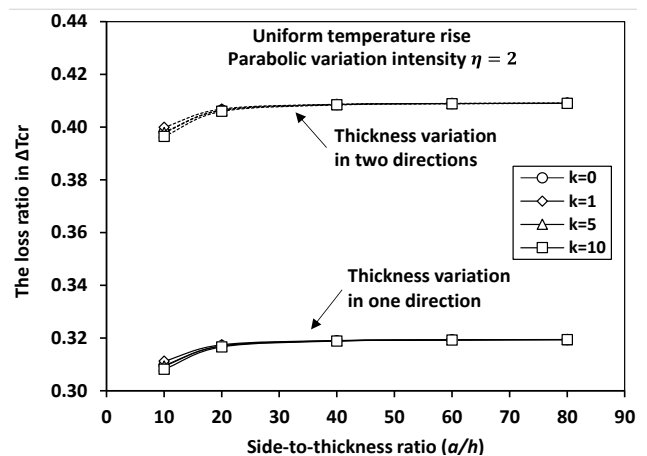


Fig. 9 Effect of side-to-thickness ratio on the loss ratio in the critical buckling temperature of FGM plate with parabolic variation intensity  $\eta = 2$  exposed to uniform temperature rise

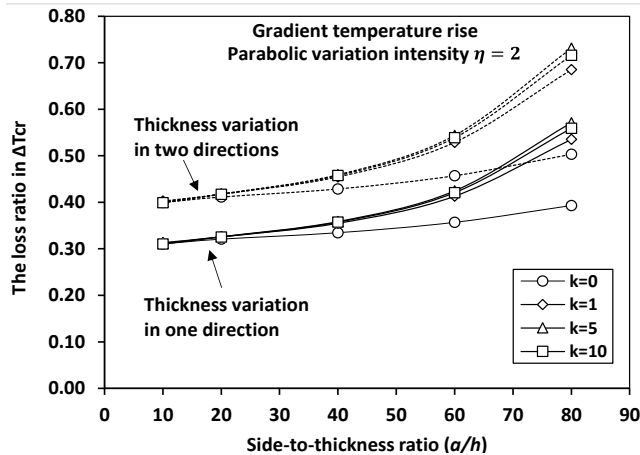


Fig. 10 Effect of side-to-thickness ratio on the loss ratio in the critical buckling temperature of FGM plate with parabolic variation intensity  $\eta = 2$  exposed to gradient temperature rise

temperature in thick plates with  $a/h < 20$  seem to have a low sensibility to the variation of the material distribution profile.

## 7. Conclusions

An investigation on the thermal stability of FGM plates is presented in this research work in order to study the degradation in the thermal buckling resistance after varying the plate thickness according a parabolic function. The derived equations are solved numerically using finite difference method to have the ability to include the thickness variation. Effect of different geometrical and material properties is studied.

According to the obtained results, applying parabolic thickness variation to simply supported FGM plates with preserving their original material volume leads to the following main conclusions:

- Varying the thickness geometry to a parabolic-concave shape with preserving its original material volume significantly reduces its critical buckling temperature especially when the variation is applied in the two longitudinal directions.
- In case of uniform temperature rise, the loss ratio in the thermal buckling resistance of homogenous plate and that of FGM plate that have the same geometric properties and thickness variation intensity, is the same. Where, under this case of thermal loading, the loss ratio in the thermal buckling resistance is not affected by the material distribution profile, except for thick plates where a minor effect is observed.
- Under gradient temperature rise, the volume fraction of the constituent materials affects the loss ratio of the thermal buckling resistance of thick plates with higher impact, compared to thin plates.
- The loss ratio in the thermal buckling resistance of FGM plates having the same material properties due to parabolic thickness variation is the same for any

applied gradient temperature profile through the thickness.

## References

- Abdelhak, Z., Hadji, L., Daouadji, T.H. and Adda, B. (2016), "Thermal buckling response of functionally graded sandwich plates with clamped boundary conditions", *Smart Struct. Syst., Int. J.*, **18**(2), 267-291.
- Bouazza, M., Tounsi, A., Adda, E.A. and Abdelkader, M. (2009), "Buckling analysis of functionally graded plates with simply supported edges", *Leonardo J. Sci.*, **8**, (15), 21-32.
- Bouguenina, O., Belakhdar, K., Tounsi, A. and Adda, B.E. (2015), "Numerical analysis of FGM plates with variable thickness subjected to thermal buckling", *Steel Compos. Struct., Int. J.*, **19**(3), 679-695.
- Bouiadjra, M.B., Houari, M.S.A. and Tounsi, A. (2012), "Thermal buckling of functionally graded plates according to a four-variable refined plate theory", *J. Therm. Stress.*, **35**(8), 677-694.
- Bourada, M., Tounsi, A. and Houari, M.S. (2012), "A new four-variable refined plate theory for thermal buckling analysis of functionally graded sandwich plates", *J. Sandw. Struct. Mater.*, **14**(1), 5-33.
- Bousahla, A.A., Benyoucef, S., Tounsi, A. and Mahmoud, S.R. (2016), "On thermal stability of plates with functionally graded coefficient of thermal expansion", *Struct. Eng. Mech., Int. J.*, **60**(2), 313-335.
- Chikh, A., Tounsi, A., Hebali, H. and Mahmoud, S.R. (2017), "Thermal buckling analysis of cross-ply laminated plates using a simplified HSDT", *Smart Struct. Syst., Int. J.*, **19**(3), 289-297.
- El-Haina, F., Bakora, A., Bousahla, A.A., Tounsi, A. and Mahmoud, S.R. (2017), "A simple analytical approach for thermal buckling of thick functionally graded sandwich plates", *Struct. Eng. Mech., Int. J.*, **63**(5), 585-595.
- El-Hassar, S.M., Benyoucef, S., Heireche, H. and Tounsi, A. (2016), "Thermal stability analysis of solar functionally graded plates on elastic foundation using an efficient hyperbolic shear deformation theory", *Geomech. Eng., Int. J.*, **10**(3), 357-386.
- Elmossouess, B., Kebdani, S., Bouiadjra, M.B. and Tounsi, A. (2017), "A novel and simple hsdst for thermal buckling response of functionally graded sandwich plates", *Struct. Eng. Mech., Int. J.*, **62**(4), 401-415.
- Fazzolari, F.A. and Carrera, E. (2014), "Thermal stability of FGM sandwich plates under various through-the-thickness temperature distributions", *J. Therm. Stress.*, **37**(12), 1449-1481.
- Fekrar, A., Zidi, M., Boumia, L., Atmane, H.A., Tounsi, A. and Adda, B.E. (2013), "Thermal buckling of AL/AL2O3 functionally graded plates based on first order theory", *Nat. Technol.*, **8**, 12-16.
- Ghomshei, M.M. and Abbasi, V. (2013), "Thermal buckling analysis of annular FGM plate having variable thickness under thermal load of arbitrary distribution by finite element method", *J. Mech. Sci. Technol.*, **27**(4), 1031-1039.
- Han, Q., Wang, Z., Nash, D.H. and Liu, P. (2017), "Thermal buckling analysis of cylindrical shell with functionally graded material coating", *Compos. Struct.*, **181**, 171-182.
- Houari, A., Benguediab, M., Bakora, A. and Tounsi, A. (2018), "Mechanical and thermal stability investigation of functionally graded plates resting on elastic foundations", *Struct. Eng. Mech., Int. J.*, **65**(4), 423-434.
- Jabbarzadeh, M., Eskandari, J.A.M.J. and Khosravi, M. (2013), "The analysis of thermal buckling of circular plates of variable thickness from functionally graded materials", *Modares Mech. Eng.*, **12**(5), 59-73.
- Jalali, S.K., Naei, M.H. and Poursolhjouy, A. (2011), "Buckling of

- circular sandwich plates of variable core thickness and FGM face sheets”, *Int. J. Struct. Stab. Dyn.*, **11**(2), 273-295.
- Kandasamy, R., Dimitri, R. and Tornabene, F. (2016), “Numerical study on the free vibration and thermal buckling behavior of moderately thick functionally graded structures in thermal environments”, *Compos. Struct.*, **157**, 207-221.
- Kettaf, F.Z., Houari, M.S.A., Benguediab, M. and Tounsi, A. (2013), “Thermal buckling of functionally graded sandwich plates using a new hyperbolic shear displacement model”, *Steel Compos. Struct., Int. J.*, **15**(4), 399-423.
- Khalfi, Y., Houari, M.S.A. and Tounsi, A. (2014), “A refined and simple shear deformation theory for thermal buckling of solar functionally graded plates on elastic foundation”, *Int. J. Comput. Methods*, **11**(5), 1350077.
- Lee, Y.H., Bae, S.I. and Kim, J.H. (2016), “Thermal buckling behavior of functionally graded plates based on neutral surface”, *Compos. Struct.*, **137**, 208-214.
- Le-Manh, T., Huynh-Van, Q., Phan, T.D., Phan, H.D. and Nguyen-Xuan, H. (2017), “Isogeometric nonlinear bending and buckling analysis of variable-thickness composite plate structures”, *Compos. Struct.*, **159**, 818-826.
- Matsunaga, H. (2009), “Stress analysis of functionally graded plates subjected to thermal and mechanical loadings”, *Compos. Struct.*, **87**(4), 344-357.
- Menasria, A., Bouhadra, A., Tounsi, A., Bousahla, A.A. and Mahmoud, S.R. (2017), “A new and simple HSDT for thermal stability analysis of FG sandwich plates”, *Steel Compos. Struct., Int. J.*, **25**(2), 157-175.
- Mozafari, H. and Ayob, A. (2012), “Effect of thickness variation on the mechanical buckling load in plates made of functionally graded materials”, *Procedia Technol.*, **1**, 496-504.
- Mozafari, H., Abdi, B. and Amran, A. (2012a), “Optimization of temperature-dependent functionally graded material based on colonial competitive algorithm”, *Appl. Mech. Mater.*, **121**, 4575-4580.
- Mozafari, H., Abdi, B., Amran, A. and Alias, A. (2012b), “Optimum critical buckling of functional graded plates under non-linear temperature by using imperialist competitive algorithm”, *Appl. Mech. Mater.*, **110**, 3429-3433.
- Mozafari, H., Ayob, A. and Alias, A. (2010a), “Influence of thickness variation on the buckling load in plates made of functionally graded materials”, *Eur. J. Sci. Res.*, **47**(3), 422-435.
- Mozafari, H., Ayob, A. and Alias, A. (2010b), “Verification of the thermal buckling load in plates plates made of functional graded materials”, *Int. J. Eng.*, **4**(5), 338-356.
- Pouladvand, M. (2009), “Thermal stability of thin rectangular plates with variable thickness made of functionally graded materials”, *J. Solid Mech.*, **1**(3), 171-189.
- Rajasekaran, S. and Wilson, A.J. (2013), “Buckling and vibration of rectangular plates of variable thickness with different end conditions by finite difference technique”, *Struct. Eng. Mech., Int. J.*, **46**(2), 269-294.
- Raki, M., Alipour, R. and Kamanbedast, A. (2012), “Thermal buckling of thin rectangular FGM plate”, *World Appl. Sci. J.*, **16**(1), 52-62.
- Szilar, R. (2004), *Theories and Applications of Plate Analysis: Classical Numerical and Engineering Methods*, John Wiley & Sons, Hoboken, NJ, USA. ISBN: 978-0-471-42989-0
- Yu, T., Yin, S., Bui, T.Q., Liu, C. and Wattanasakulpong, N. (2017), “Buckling isogeometric analysis of functionally graded plates under combined thermal and mechanical loads”, *Compos. Struct.*, **162**, 54-69.
- Zenkour, A.M. and Mashat, D.S. (2010), “Thermal buckling analysis of ceramic-metal functionally graded plates”, *Nat. Sci.*, **2**(9), 968-978.
- Zenkour, A.M. and Sobhy, M. (2010), “Thermal buckling of various types of FGM sandwich plates”, *Compos. Struct.*, **93**(1), 93-102.
- Zhao, X., Lee, Y.Y. and Liew, K.M. (2009), “Mechanical and thermal buckling analysis of functionally graded plates”, *Compos. Struct.*, **90**(2), 161-171.

CC